Composites Engineering, Vol. 3, Nos 7-8, pp. 585-599, 1993.
Printed in Great Britain.

0961-9526/93 $6.00 + .00

MULTIDISCIPLINARY OPTIMIZATION AND DESIGN VARIABLE SENSITIVITY OF HELICOPTER ROTOR BLADES USING A COMPOSITE BOX BEAM MODEL

ADITI CHATTOPADHYAY and THOMAS R. MCCARTHY
Department of Mechanical and Aerospace Engineering, Arizona State University, Tempe, AZ 85287-6106, U.S.A.

Abstract—The paper addresses a fully integrated optimization procedure, for helicopter rotor blades, with the coupling of blade dynamics, aerodynamics, aeroelasticity and structures. The goal is to reduce vibratory shear forces at the blade root with constraints imposed on critical dynamic, aerodynamic, aeroelastic and structural design requirements. The blade is modeled with a composite box beam as the principal load carrying member. Nonlinear chord and twist variations are assumed. A wide range of both structural and aerodynamic design variables are used along with several subsets to determine the sensitivity of the design variables on the optimum design. The optimization problem is formulated with two objective functions and the Kreisselmeier-Steinhauser (K-S) function approach for multiple design objectives is used. A nonlinear programming technique and an approximate analysis procedure are used for optimization. The procedure yields substantial reductions in the vibratory root forces and moments along with significant improvements in the remaining design requirements. Comparisons with previous work where isotropic beam elements were used indicate that the use of a composite box beam yields significant improvements in the blade design. Results are presented for several different cases of design variable vectors and are compared with a baseline, or reference blade.

NOMENCLATURE

c	chord (ft)
f_r	3/rev radial shear (lb)
f_x	3/rev inplane shear (lb)
f_z	4/rev vertical shear (lb)
g	constraint functions
k	stiffness matrix
m_c	3/rev torsional moment (lb-ft)
m_x	3/rev flapping moment (lb-ft)
m_z	4/rev lagging moment (lb-ft)
p	chord distribution shape parameter
t_{ply_ψ}	thickness of ply with orientation ψ
v	horizontal displacement
w	vertical displacement
w_{tj}	nonstructural weight at jth node and 2.5% chord location (lb)
w_{cj}	nonstructural weight at jth node and 40% chord location (lb)
x, y, z	reference axes
$\bar{y}$	nondimensional radial location
AI	autorational inertia (lb-ft^2)
C_T	thrust coefficient
C_p	power coefficient
EI_{xx}	logging stiffness (lb-ft^2)
EI_{zz}	flapping stiffness (lb-ft^2)
F_k	objective functions
F_{k_0}	values of F_k at the beginning of an iteration
GJ	torsional stiffness (lb-ft^2)
K	total number of constraints and objective functions
N_{CON}	number of constraints
N_{DV}	number of design variables
N_{OBJ}	number of objective functions
N_{SEG}	number of blade segments
N_{MEM}	number of box beam structural members
R	blade radius (ft)
T	thrust (lb)
W	total blade weight (lb)
β	chord distribution shape parameter

δ	twist shape parameter
λ	inverse taper ratio
μ	advance ratio
ρ	K-S function multiplier
θ	blade twist (°)
σ	thrust-weighted solidity
τ	twist ratio
ψ	ply orientation
Φ	design variable vector
Ω	rotor angular velocity (r.p.m.)

Subscripts

max	maximum value
r	value at the blade root
ref	reference blade value
t	value at the blade tip
L	lower bound
U	upper bound

INTRODUCTION

Rotary wing aircraft design is truly multidisplinary in nature and therefore an integration of the necessary disciplines is essential for an optimization procedure to be meaningful. The necessity of such integrated multidisciplinary optimization procedures for helicopter rotor blades is currently being recognized. Celi and Friedmann (1987) addressed the coupling of dynamic and aeroelastic criteria with quasisteady airloads for minimization of the 4/rev vertical hub shear for a four-bladed rotor with straight and swept tips. Lim and Chopra (1988) coupled a comprehensive aeroelastic analysis code with the nonlinear optimization algorithm CONMIN (Vanderplaats, 1973) to reduce vibratory hub loads of a hingeless four-bladed rotor in order to reduce vibration without compromising aeroelastic stability in forward flight. However in these studies, only quasisteady airloads were used. An integrated aerodynamic/dynamic optimization procedure was presented by Chattopadhyay *et al.* (1991). The 4/rev vertical hub shear and blade weight of a four-bladed articulated rotor were minimized. A modified Global Criteria approach was used to formulate the multiobjective optimization problem. The integration of aerodynamic loads and dynamics was achieved by coupling the comprehensive helicopter analysis code CAMRAD (Johnson, 1980b) with CONMIN and an approximate analysis technique. The program CAMRAD permitted the calculation of actual airloads. The use of this program within the optimization loop allowed for the effects of design variable changes during optimization and the associated changes in airloads to be included in the design process. Chattopadhyay and Chiu (1990) extended the work of Chattopadhyay *et al.* (1991) to include the other five vibratory hub forces and moments in the form of objective functions and/or constraints. He and Peters (1990) performed a combined structural, dynamic and aerodynamic optimization of rotor blades using a simple box beam model to represent the structural component in the blade. The blade performance was optimized using the power required in hover as the objective function and constraints were imposed on natural frequencies, blade stress and fatigue life. However, an assumed blade loading was used and the optimization procedure was decoupled into two levels. Straub *et al.* (1991) addressed the problem of combined aerodynamic performance and dynamic optimization, at both forward flight and hover flight conditions, by using the comprehensive rotor analysis code CAMRAD/JA (Johnson, 1988). A linear combination of the objective functions was used to formulate the multiple design objective problem.

Chattopadhyay and McCarthy (1991, 1993) recently addressed multiobjective formulation procedures in the context of a nonlinear rotor blade optimization problem. Firstly (Chattopadhyay and McCarthy, 1991), the optimum design problem of Chattopadhyay *et al.* (1991) was solved using three different multiobjective formulation techniques, the modified Global Criterion approach, the Minimum Sum Beta (Min $\Sigma\beta$) approach (Weller and Davis, 1986) and the Kreisselmeier-Steinhauser (K-S) function approach (Sobieski

et al., 1988). This work was later extended (Chattopadhyay and McCarthy, 1993) by replacing the generic design variables of the previous work (Chattopadhyay and McCarthy, 1991) with a detailed structural model. Also a constraint on the offset of elastic axis from mass center of gravity was used as a first step towards the inclusion of an aeroelastic stability constraint. The Min $\Sigma\beta$ and the K-S function approaches were used to solve the optimization problem. Very recently, multidisciplinary optimization efforts have also been initiated to investigate the design of high speed rotorcraft (Chattopadhyay and Narayan, 1992; McCarthy, 1992).

In the present paper, a further step towards the integrated optimization procedure for helicopter rotor blade design is taken by including a complete aeroelastic stability analysis, based on Floquet theory (Johnson, 1980), inside the closed-loop optimization procedure. The isotropic beam used by Chattopadhyay and McCarthy (1993) is replaced by a composite box beam which is the principal load carrying member inside the blade. The box beam is used to investigate the influence of composites on blade vibration and aeroelasticity. The box beam analysis is based on the model developed by Smith and Chopra (1991). Since the proper choice of design variables is critical in an optimization process, several combinations of design variables are used and their effects on the optimum design are investigated. The reference blade chosen for this study is a modified wind tunnel model of an existing advanced helicopter, which is a four-bladed articulated rotor with a rigid hub.

OPTIMIZATION FORMULATION

The optimization problem can be mathematically posed as follows.

Minimize:

$$F_k(\Phi_n) \qquad k = 1, 2, \ldots, N_{OBJ} \qquad \text{objective functions}$$
$$n = 1, 2, \ldots, N_{DV}$$

subject to:

$$g_j(\Phi_n) \leq 0 \qquad j = 1, 2, \ldots, N_{CON} \qquad \text{inequality constraints}$$
$$\Phi_{nL} \leq \Phi_n \leq \Phi_{nU} \qquad \text{side constraints,}$$

where N_{OBJ} denotes the number of objective functions, N_{DV} is the number of design variables and N_{CON} is the total number of constraints. The subscripts L and U denote lower and upper bounds, respectively, on the design variable Φ_n. In this paper, since a multidisciplinary design problem is addressed, the objective functions, the constraints and the design variables are carefully selected from each of the disciplines considered.

Multiobjective optimization

Due to the fact that the optimization problem involves more than one design objective, the objective function formulation is more complicated than single objective optimization problems. From previous studies (Chattopadhyay and McCarthy, 1991, 1993) it was found that the K-S function approach for formulating multiobjective problems is well suited in the highly nonlinear rotor blade design optimization problem. Therefore the K-S function approach is used in this study.

Using the K-S function approach, the original objective functions are transformed into reduced objective functions which assume the following form.

$$F_k^*(\Phi) = \frac{F_k(\Phi)}{F_{k_0}} - 1 - g_{\max} \leq 0 \qquad K = 1, 2, \ldots, N_{OBJ}, \tag{1}$$

where F_{k_0} represents the value of the original objective function, F_k, calculated at the beginning of each iteration. The quantity $g_{\max}$ is the value of the largest constraint corresponding to the original constraint vector, $\mathbf{g}_j(\Phi)$ and is held constant during each iteration. These reduced objective functions are analogous to the previous constraints. Therefore, a new constraint vector $\mathbf{g}_m(\Phi)$, $m = 1, 2, \ldots, M$, is introduced, where $M = N_{CON} + N_{OBJ}$.

This constraint vector includes the original constraints of the problem as well as the constraints introduced by eqn (1). The new objective function to be minimized is then defined, using the K-S function, as follows.

$$\tilde{F}(\Phi) = f_{\max} + \frac{1}{\rho} \sum_{m=1}^{M} e^{\rho(g_m(\Phi) - f_{\max})}, \tag{2}$$

where $f_{\max}$ is the largest constraint corresponding to the new constraint vector, $\mathbf{g}_m(\Phi)$, and in general is not equal to $g_{\max}$. The optimization procedure is as follows. Initially in an infeasible design space, where the original constraints are violated, the constraints due to the reduced objective functions [eqn (1)] are satisfied, i.e. $g_{\max}$ is negative. Once the original constraints are satisfied, the constraints due to the reduced objective functions become violated. When this happens, the optimizer attempts to satisfy these constraints and in doing so, minimizes the original objective functions (F_k). The multiplier ρ is analogous to a draw-down factor where ρ controls the distance from the surface of the K-S objective function to the surface of the maximum constraint function. When ρ is large, the K-S function closely follows the surface of the largest constraint function. When ρ is small, the K-S function includes contributions from all violated constraints. The design variable vector Φ remains unchanged using this multiobjective function formulation technique.

AERODYNAMIC MODEL

A wind tunnel blade model of an existing advanced four-bladed articulated rotor is used as a reference blade. In this section, details of the aerodynamic planform modeling, used to formulate the optimization problem, is explained. The normalized chord distribution, $\bar{c}(y)$, is defined to have spanwise chord variation as follows:

$$\bar{c}(y) = \frac{c(y)}{c_r} = [1 + \bar{y}(\lambda - 1)][1 - \bar{y}^{1/\beta}]^p, \tag{3}$$

where c_r is the root chord, $\bar{y}$ is the nondimensional radius and λ is the inverse taper ratio, i.e. $\lambda = c_t/c_r$ where c_t is the tip chord. The tip shape parameter is denoted p and defines the blade shape at the tip. The tip length parameter is denoted α and defines the amount of tip taper. Both α and p are defined to be strictly positive.

The blade twist, $\bar{\theta}(y)$, normalized with respect to the root twist θ_r, is defined to have the following spanwise variation:

$$\bar{\theta}(y) = \frac{\theta(y)}{\theta_r} = 1 + \bar{y}^{\delta}(\tau - 1). \tag{4}$$

In the above equation, τ is the twist ratio, given by $\tau = \theta_t/\theta_r$, where θ_t is the tip twist and δ is the twist shape parameter which is defined to be positive. The physical significance of the twist shape parameter, δ, is such that with $\tau = 0$ the twist distribution is concave for $0 < \delta < 1$ and convex when $\delta > 1$. The limiting case of $\delta = 1$ indicates linear twist. The chord and twist distributions are chosen to closely represent actual distributions for helicopter rotor blades.

COMPOSITE STRUCTURAL MODELS

The load carrying member of the rotor is modeled as a single-celled composite box beam (Fig. 1). Spanwise nonstructural tuning masses are located at both 2.5 and 40% chord locations. In addition to these nonstructural masses, the weights of the honeycomb structure and the blade skin are also included in the total weight and center of gravity calculations.

The outer dimensions of the box beam (Fig. 2) are constants based on percentage chord at the 90% span radial location [$\bar{y} = 0.90$ in eqn (3)]. The beam is modeled with unequal vertical and horizontal wall thicknesses and the beam cross section is described by stretching, bending, twisting, shearing and torsion related warping (Smith and Chopra, 1991).

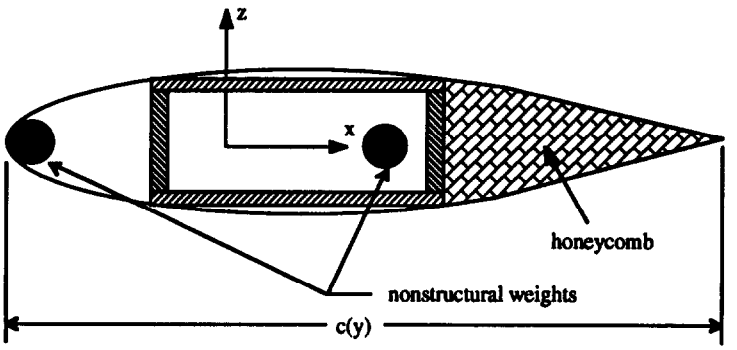

Fig. 1. Blade cross section.

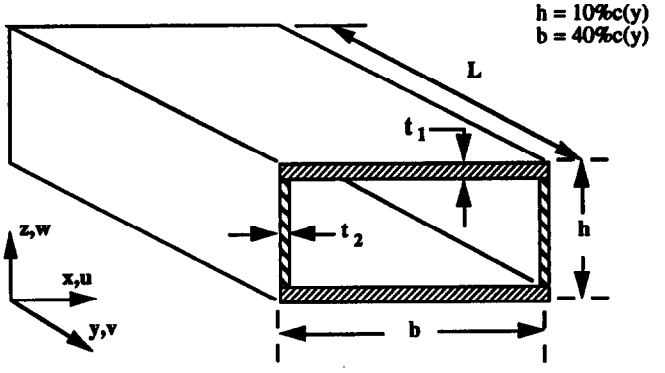

Fig. 2. Single cell composite box beam.

The box beam walls are made of layers of laminated orthotropic composite plies. A symmetric (90°) four ply arrangement, with respect to beam axis, is used for the horizontal wall and a symmetric arrangement $[(0°/90°)_2/0°/(90°/0°)_2]$ is used for the vertical wall to model the reference blade. These ply arrangements are selected to closely model the reference blade stiffness distributions. The total thickness of plies with a given orientation, ψ, is denoted t_{ply_ψ}.

The bending stiffnesses are then calculated as follows:

$$\begin{Bmatrix} m_z \\ m_x \\ T \end{Bmatrix} = \begin{bmatrix} k_{66} & 0 & k_{46} \\ 0 & k_{55} & k_{45} \\ k_{46} & k_{45} & k_{44} \end{bmatrix} \begin{Bmatrix} v'' \\ w'' \\ \alpha' \end{Bmatrix}, \tag{5}$$

where m_z and m_x are the lagging and flapping moments, respectively, T is the torsional moment and k is the stiffness matrix. The horizontal and vertical displacements are denoted by v and w, respectively and α is the pitch angle (see Fig. 2).

OPTIMIZATION IMPLEMENTATION

In this section, a detailed description of the optimization problem, in terms of the objective functions, constraints and design variables, is provided. This is followed by a description of the optimization algorithm and the approximate analysis procedure.

Objective functions

For a four-bladed articulated rotor in forward flight, the vibratory hub loads (in the fixed frame) occur at the blade passing frequency of 4/rev. In the rotating frame these include contributions from the 3 and 5/rev loads as well (Johnson, 1980). However, the magnitudes of the 5/rev loads are generally small compared to the 3/rev loads and are therefore ignored. A rotor with low vibratory hub loads will produce low vibration in the airframe, therefore minimization of hub loads is a proper step. Therefore, in this

problem, since the magnitudes of the 4/rev vertical shear (f_z) and the 3/rev inplane shear (f_x), at the blade root, are the most significant, they are used as objective functions to be minimized.

Constraints

The constraints are carefully selected from each of the disciplines considered. A detailed description of these follows.

Dynamic constraints. To avoid any degradation of the remaining vibratory loads, not included as objective functions, upper bound constraints are imposed on these forces and moments. These constraints are summarized below:

(i) 3/rev radial shear; $f_r \leq f_{r_U}$;
(ii) 4/rev lagging moment; $m_z \leq m_{z_U}$;
(iii) 4/rev flapping moment; $m_x \leq m_{x_U}$;
(iv) 4/rev torsional moment; $m_c \leq m_{c_U}$.

Results of previous research (Chattopadhyay and McCarthy, 1993) indicated that the inclusion of the above constraints was sufficient in maintaining the natural frequencies away from critical values. Therefore, no additional constraints are imposed on the natural frequencies.

Aerodynamic constraints. It is important to ensure that the power required by the optimum blade is no greater than the reference blade. It is also essential that the optimum rotor maintains the same lifting capability as the reference rotor. Therefore the aerodynamic constraints are formulated as follows:

(v) $C_P \leq C_{P_U}$;
(vi) $T \geq T_L$.

Structural constraints. An upper bound constraint is imposed on the total blade weight (W) to avoid the usual weight penalties associated with the vibration reduction problem. Also, a lower bound is imposed on the autorotational inertia (AI) to ensure that the rotor has sufficient inertia to autorotate in the event of engine failure. These structural constraints are summarized below:

(vii) $W \leq W_U$;
(viii) $AI \geq AI_L$.

Aeroelastic constraints. It is important to impose aeroelastic stability constraints to prevent any degradation of the rotor stability, after optimization, especially since the blade mass and stiffnesses are being altered. The stability constraints are expressed as follows:

(ix) $\alpha_k \leq -\nu_k \qquad k = 1, 2, \ldots, K.$

Here K represents the total number of modes considered and α_k is the real part of the stability root defined as:

$$\alpha_k = \frac{1}{2\pi} \ln \sqrt{(\lambda_k^R)^2 + (\lambda_k^I)^2}, \tag{6}$$

where λ_k are the eigenvalues of Floquet transition matrix and the superscripts R and I represent the real and imaginary parts, respectively. The quantity ν_k denotes a minimum allowable blade damping and is a positive number.

Design variables

Three different case studies are performed to investigate the sensitivity of design variable selection. A description of these cases follows.

Case I. The first design variable vector consists only of the aerodynamic variables. Therefore, the parameters defining the chord and twist distributions [eqns (1), (2)] are used and are described below:

(i) chord distribution parameters; c_r, $\tilde{\lambda}$, α and p;
(ii) twist distribution parameters; θ_r, τ and δ.

Case II. The second design variable vector comprises structural variables only. Therefore, the parameters that define the blade structural properties are used. This vector is defined as follows:

(i) ply thickness, t_{ply_ψ};
(ii) nonstructural weights at two locations (2.5 and 40.0% chord, see Fig. 1); w_{t_j} and w_{c_j}; $j = 1, 2, \ldots, \text{N}_{\text{SEG}}$.

Case III. Finally a design variable vector comprising both aerodynamic and structural variables is used. Therefore, all the variables used in Cases I and II are used simultaneously in this case.

Optimization and approximation

The optimization algorithm used is the program CONMIN, which is an optimizer based upon the method of feasible directions. Since the use of exact analyses for the calculations of the objective functions and constraints during each iteration of CONMIN is computationally prohibitive, an approximate analysis technique, based upon a two-point exponential approximation developed by Fadel *et al.* (1991) is used. This technique assumes its name from the fact that the exponent used in the expansion is based upon gradient information from the previous design point and is formulated as follows:

$$\hat{F}(\Phi) = F(\Phi_0) + \sum_{n=1}^{\text{NDV}} \left[\left(\frac{\varphi_n}{\Phi_{0_n}} \right)^{p_n} - 1.0 \right] \frac{\Phi_{0_n}}{p_n} \frac{\partial F(\Phi_0)}{\partial \Phi_n}, \tag{7}$$

where

$$p_n = \frac{\ln\{(\partial F(\Phi_1)/\partial \Phi_n)/(\partial F(\Phi_0)/\partial \Phi_n)\}}{\ln(\Phi_{1_n}/\Phi_{0_n})} + 1.0. \tag{8}$$

The quantity Φ_1 refers to the design variable vector from the previous iteration and the quantity Φ_0 denotes the current design vector. A similar expression is obtained for the constraint vector. The exponent p_n can be considered as a "goodness of fit" parameter, which explicitly determines the trade-offs between traditional and reciprocal Taylor series based expansions (also known as a hybrid approximation technique). It can be seen, from eqn (7), that in the limiting case of $p_n = 1$, the expansion is identical to the traditional first order Taylor series and with $p_n = -1$ the two-point exponential approximation assumes the reciprocal expansion form. The exponent is therefore defined to lie within this interval, such that if $p_n > 1$, it is set identically equal to one, and if $p_n < -1$, it is set equal to -1. From eqns (7), (8), it is obvious that singularities can arise while using this method, therefore, care must be taken to avoid such points. In the present paper, the approximation method used is reverted to the linear first order Taylor series based approach at such singular points.

ANALYSIS

In this section, a description of the analysis procedures, coupled within the optimization process, is given.

Structural analysis

The structural analysis of the rotor blade is performed using a recently developed inhouse code that determines the section properties of the rotor blade. The code models

a single cell composite box beam (Fig. 2), symmetric about the x and z axes, which is assumed to carry all loads within the rotor. It is assumed that the flatwise, chordwise and torsional stiffnesses of the blade are provided solely by the box beam.

Dynamic, aerodynamic and aeroelastic analyses

The program CAMRAD is used for both blade dynamic and aerodynamic analyses. The program calculates the section loading from the airfoil two-dimensional aerodynamic characteristics. It uses the lifting line or blade element approach and has corrections for yawed and three-dimensional flow effects. The following assumptions are made while running the code: uniform inflow, yawed flow on the rotor and unsteady aerodynamics. The blade is trimmed within CAMRAD at each cycle so that the intermediate designs, which are feasible designs, represent trimmed configurations. A wind tunnel trim option is used and the rotor lift and drag, each normalized with respect to solidity, and the flapping angle are trimmed using the collective pitch, the cyclic pitch and the shaft angle. The optimized rotor is trimmed to the same value of the thrust coefficient (C_T) as the reference rotor using a variable trim procedure developed previously by Chattopadhyay and McCarthy (1993). The blade response is calculated, in CAMRAD, using rotating free-vibration modes equivalent to a Galerkin analysis. Ten bending modes, of which seven are flapping dominated and three are lead–lag dominated, and three torsion modes are calculated. Main blade responses of up to 8/rev are included. Therefore, eight harmonics of the rotor revolution are retained in the airloads calculations. The vibratory shear forces and moments are calculated based upon the airloads information obtained from the aerodynamic analysis. The aeroelastic stability analysis is performed using Floquet theory for periodic state equations as implemented in CAMRAD. Four bending degrees of freedom and one torsional degree of freedom are used for the stability analysis.

RESULTS

The optimization procedure is applied to the reference blade which has a radius, $R = 4.685$ ft and a rotational velocity, $\Omega = 639.5$ rpm. The rotor is optimized for an advance ratio, $\mu = 0.3$. The blade is discretized into 10 segments (i.e. $N_{SEG} = 10$). A total of seven design variables are used in the aerodynamic design variable case (Case I). In the structural design variable case (Case II) a total of 23 design variables are used. In Case III (integrated aerodynamic and structural design variables) a total of 30 design variables are used. The maximum number of cycles are necessary in Case I, where a cycle comprises analysis and optimization. After a total of 72 cycles (2.3 C.P.U. h on a Cray X-MP/116se supercomputer) a truly converged feasible solution is not achieved. The 3/rev torsional moment is violated slightly (2.1%). However, since this violation is not critical and since the remaining constraints are well satisfied, the solutions of Case I are presented and are compared against those obtained from Cases II and III. Only 17 cycles are required for convergence in Case II, which is equivalent to 1.5 C.P.U. h on the Cray, and 25 cycles, equivalent to 2.7 C.P.U. h, are required for convergence in Case III. The constraints are well satisfied in these two cases.

The optimum results are presented in Tables 1 and 2 and in Figs 3–12. It can be seen from Table 1 and Fig. 3, that significant reductions in the individual objective functions (f_z and f_x) are obtained in all three cases. The 4/rev vertical shear (f_z) is reduced by 26.1% in Case I, 38.3% in Case II and 31.2% in Case III. The 3/rev inplane shear (f_z) is reduced by 16.1% in Case I, 33.6% in Case II and 22.5% in Case III. In Case I, the 3/rev radial shear (f_r) and flapping moment (m_x) are reduced from the reference values by 17.5 and 3.2%, respectively and the 4/rev lagging moment is reduced by less than 1%. As mentioned earlier, the constraint on the 3/rev torsional moment (m_c) is not strictly satisfied in this case. In Case II, f_r, m_z and m_x are reduced by 30.2, 47.0 and 79.9%, respectively. The 3/rev torsional moment is reduced by 8.6%. In Case III, f_r, m_z and m_x are reduced by 19.8, 6.1 and 5.2%, respectively. The 3/rev torsional moment (m_c) is reduced by 8.2%. As expected, the largest reductions in the vibratory forces occur in

Table 1. Summary of optimization results

	Reference blade	Bounds		Optimum		
		lower	upper	Case I	Case II	Case III
Objective functions						
4/rev f_z (lb)	0.501	—	—	0.371	0.309	0.345
3/rev f_x (lb)	2.89	—	—	2.42	1.92	2.23
Constraints						
AI (lb-ft^2)	31.0	31.0	—	31.0	34.2	31.3
W (lb)	4.79	—	4.79	4.78	4.77	4.79
3/rev f_r (lb)	2.12	—	2.12	1.75	1.48	1.70
4/rev m_z (lb-ft)	0.602	–	0.602	0.600	0.319	0.565
3/rev m_c (lb-ft)	0.594	—	0.594	0.575	0.543	0.545
3/rev m_x (lb-ft)	0.135	—	0.135	0.138†	0.0272	0.128
T (lb)	282.0	282.0	—	282.0	282.0	282.0
C_P	0.000510	—	0.000510	0.000458	0.000499	0.000464
Solidity						
σ	0.116	—	—	0.116	0.116	0.116
Trim						
C_T/σ	0.0591	—	—	0.0591	0.0591	0.0591

† Violated constraint

Table 2. Summary of design variables

	Design variables	Reference	Optimum		
			Case I	Case II	Case III
Ply thickness (in.)	(90°)hor	0.01	—	0.0229	0.0105
	(0°)ver	0.01	—	0.0138	0.0104
	(90°)ver	0.01	—	0.0123	0.00990
Root chord	c_r (ft)	0.450	0.452	—	0.434
Chord shape	λ	1.00	0.990	—	1.08
Parameters	α	0.0100	0.0104	—	0.0100
	p	0.0100	0.00942	—	0.00999
Root twist	θ_r (°)	12.0	10.6	—	9.64
Twist shape	τ	−0.333	−0.333	—	−0.326
Parameters	δ	1.00	0.726	—	0.874

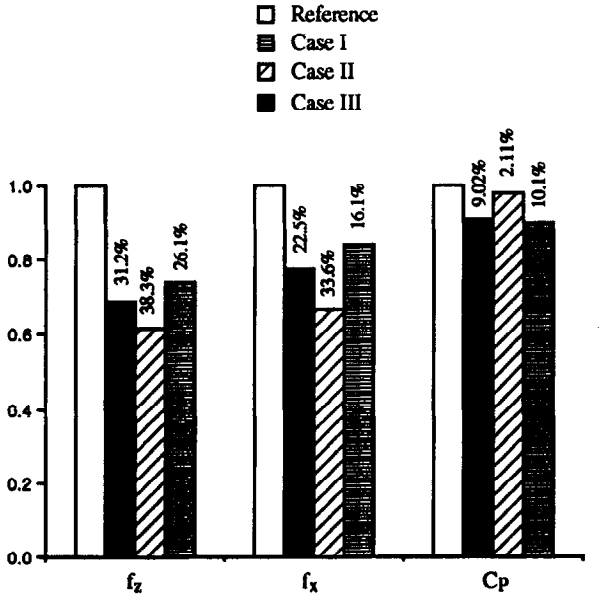

Fig. 3. Comparison of optimum results.

Case II which comprises structural design variables only. This is followed by Case III, which comprises aerodynamic and structural variables.

It can be seen from Fig. 3 that the reduction in the coefficient of total power (C_P) is maximum (10.1%) in Case I, which represents the aerodynamic design variable case, followed by Case III (9.0%) and Case II (2.1%). Case I represents the aerodynamic design variable case and therefore yields the least reductions in the vibratory forces and Case II which represents the structural design variable case yields the lowest reduction in the aerodynamic performance parameter, C_P.

The thrust (T) of the optimum rotor is at the prescribed lower bound in each of the three cases. In all three cases, the total blade weight (W) is either slightly reduced (less than 1%) or is active. The autorotational inertia (AI) is active in Case I and is increased by 10.3 and 1.0%, respectively, in Cases II and III. It is interesting to note that the thrust-weighted solidity (σ) of the optimum rotors remains equal to the reference blade although it is allowed to vary during optimization in Cases I and III.

The design variables, before and after optimization, are presented in Table 2. There are significant increases in the ply thicknesses in Case II, from reference to optimum. For example, the thickness of the 90° ply in the horizontal wall increases by 229% and in the vertical wall, the thicknesses of the 0° and the 90° plies increase by 37.6 and 22.8%, respectively. In Case III, the 90° ply in the horizontal wall increases by 4.5% and the 0° ply in the vertical wall increases by 4.4%. The large increases in ply thickness in Case II are attributable to the fact that in this case, since aerodynamic parameters are not altered during optimization, less than ideal twist and chord distributions exist which necessitate a stiffer blade than the optimum blade of Case III in which aerodynamic variables are included.

The blade chord length distributions are shown in Fig. 4. In Case I, the root chord (c_r) is slightly increased (less than 1%) from the baseline, whereas in Case III, c_r is reduced by 4.3%. Therefore it is logical that the inverse taper ratio (λ) is reduced from the reference Case I ($\lambda = 0.990$) and is slight increased in Case III ($\lambda = 1.08$). The chord distribution in Case I is very similar to the reference chord distribution due to the fact that the aerodynamic design variables used in this case are only weakly connected to the objective functions and majority of the constraints.

The blade stiffness distributions are presented in Figs 6 and 7. Note that the spanwise variations of the stiffnesses are assumed to be constant. The lagging stiffness (EI_{xx}) is shown in Fig. 6. In Case I, this stiffness reduces by 1.4%, whereas in Cases II and III there are significant increases (15.0 and 37.0%, respectively). Figure 7 shows the flapping (EI_{zz}) and torsional stiffness (GJ) distributions. In Case I, EI_{zz} and GJ decrease by 1.4 and 1.3%, respectively. Significant increases of 73.6 and 114 are achieved in the EI_{zz} values

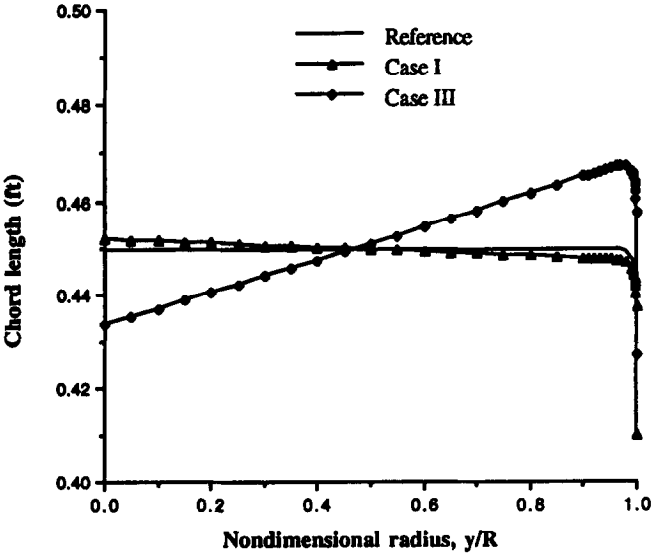

Fig. 4. Chord length distribution.

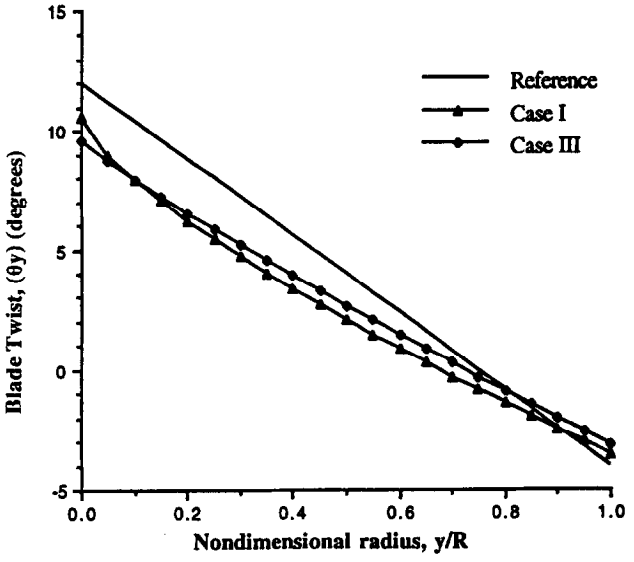

Fig. 5. Twist distribution.

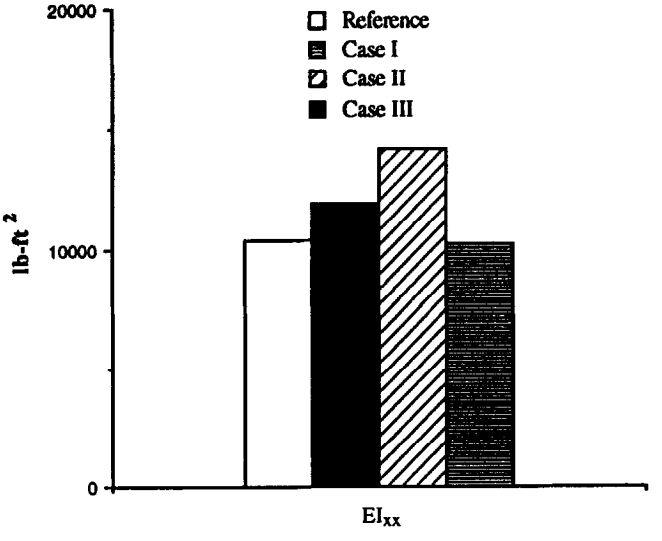

Fig. 6. Lagging stiffness distribution.

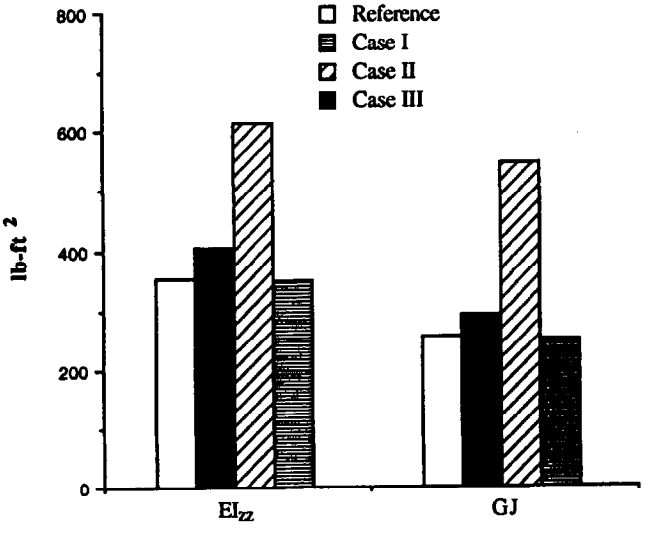

Fig. 7. Flapping and torsional stiffnesses.

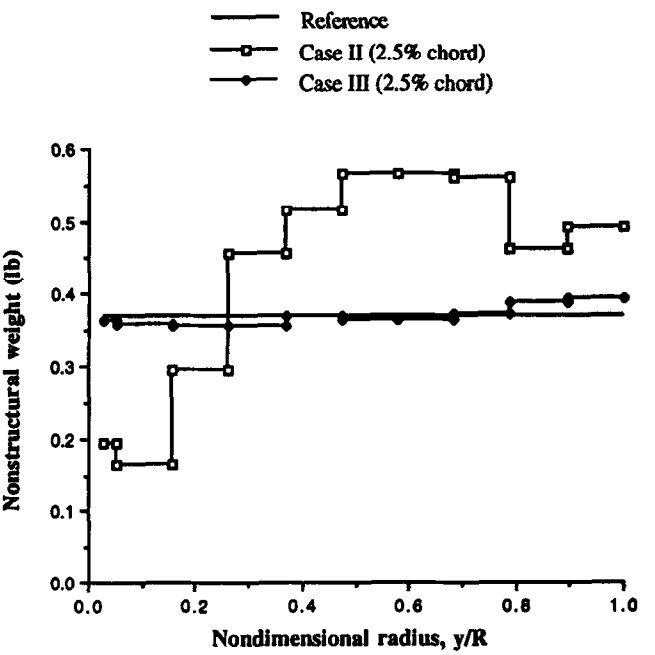

Fig. 8. Nonstructural weight distribution at 2.5% chord.

in Cases II and III, respectively. The corresponding increases in GJ are 114 and 15.0%. The large increases in the stiffnesses in Cases II and III, are due to the presence of the structural design variables. The inclusion of these design variables allows blade stiffening to be the primary mechanism of vibration reduction.

The nonstructural weight distributions (w_{t_j} and w_{c_j}, $j = 1, 2, \ldots, N_{SEG}$) for Cases II and III are shown in Figs 8 and 9. In both cases the general trend is to reduce the weights at inboard locations and to increase them towards the blade tip. This is done to satisfy both the weight and autorotational constraints which are conflicting in nature. There is also a general trend in reducing the nonstructural weights at the 40% chord location (w_c) to values lower than those at the 2.5% chord location (w_t). This can be explained as an effort to improve blade stability by moving the blade center of gravity forward. These trends are most prominent in Case II.

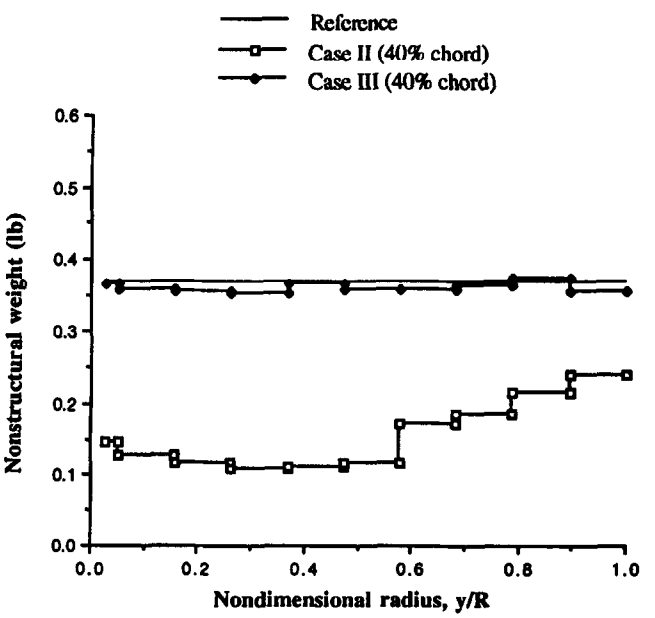

Fig. 9. Nonstructural weight distribution at 40% chord.

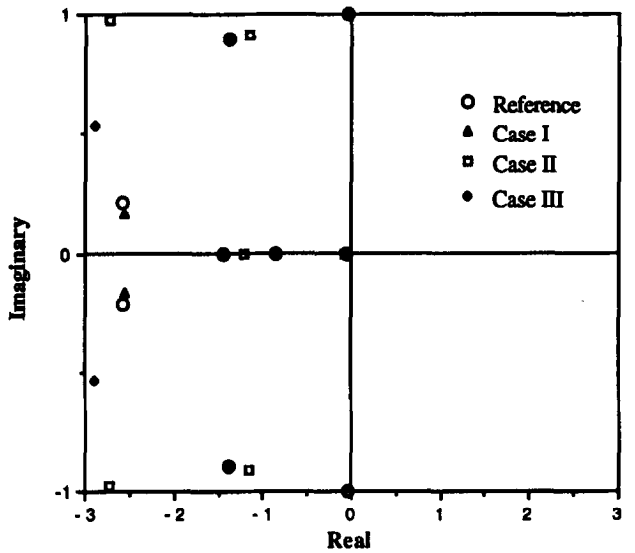

Fig. 10. Root locus plot of aeroelastic stability poles.

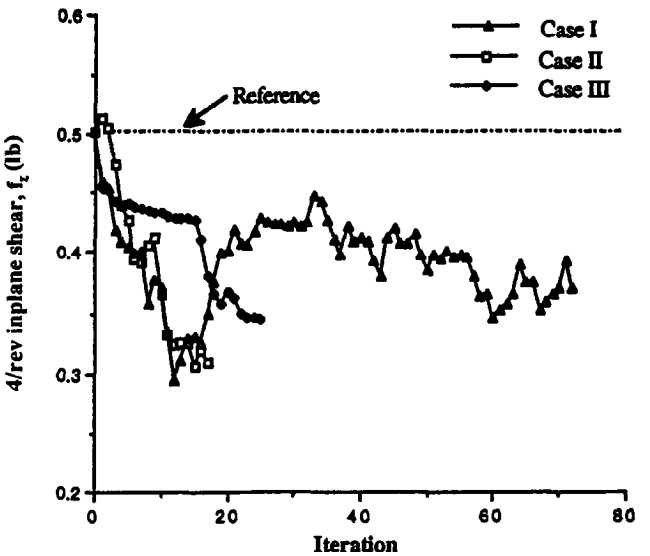

Fig. 11. 4/rev vertical shear convergence history.

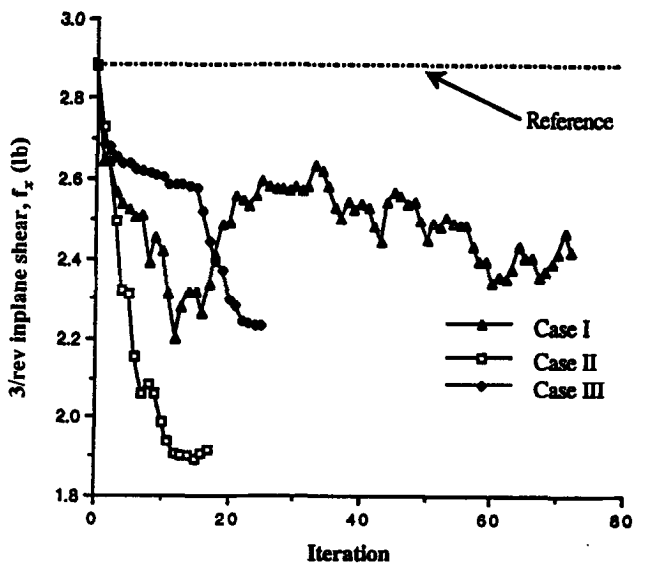

Fig. 12. 3/rev inplane shear convergence history.

The stability roots for all three cases are shown in Fig. 10. All three optimum blades and the reference blade consist of negative poles indicating that blade aeroelastic stability has been maintained after optimization. The individual objective function iteration histories for f_z and f_x are shown in Figs 11 and 12. In Cases II and III, f_z and f_x decrease nearly monotonically, whereas in Case I, their values are highly oscillatory. This once again indicates that the aerodynamic design variables are not as effective in reducing vibratory loads as the structural design variables.

The results, when compared to the previous studies performed using an isotropic beam model (Chattopadhyay and McCarthy, 1991 and 1993) indicate very significant improvements in blade vibrations. This shows that the use of composites is not just advantageous from the point of view of weight savings, but also provides the benefit of extension-twist and extension-bending coupling as mechanisms for reduced vibration.

CONCLUDING REMARKS

A fully integrated optimization procedure has been developed for the design of helicopter rotor blades. Blade dynamic, aerodynamic, aeroelastic and structural design requirements are coupled within a closed-loop optimization process. The 4/rev vertical and the 3/rev inplane shears, at the blade root are reduced using the K-S function approach of formulating multiobjective problems. The optimizer comprises a nonlinear programming technique and an approximate analysis procedure. Three different sets of design variables are used to study their effects on the optimization. The procedure yields significant design improvements. The following specific observations have been made.

(1) Large reductions were obtained in the original objective functions. The most significant reductions were obtained in Case II followed by Case III indicating that the structural design variables were most effective in reducing the vibratory stresses and moments. This indicates that the use of composites is a very effective means of vibration reduction.
(2) Comparisons with previous research where isotropic box beam analyses were used, show larger reductions in vibration, indicating the advantage of the composite box beam.
(3) The influence of the aerodynamic design variables (twist in particular) was demonstrated through significant reductions in the total power coefficient which was reduced by 10.1, 2.1 and 9.0%, in Cases I, II and III, respectively.
(4) The aerodynamic design variable vector proved to be the most effective in reducing the total coefficient of power. However, it was difficult to completely satisfy the constraint on the torsional moment using this case.
(5) The combined design variable vector was the most effective for the overall integrated problem and also provided the smoothest convergence.
(6) Convergence to optimum was the fastest in Case II indicating the strong influence of the structural design variables to the objective functions and constraints.

Acknowledgements—The author's acknowledge that the research was partially supported through a grant from the NASA Ames Research Center, Grant number NAG2-771.

REFERENCES

Celi, R. and Friedmann, P. P. (1987). Efficient structural optimization of rotor blades with straight and swept tips. *Proc. 13th European Rotorcraft Forum*, September, Arles, France, No. 3-1.

Chattopadhyay, A. and Chiu, Y. D. (1990). Details of an enhanced aerodynamic/dynamic optimization procedure for helicopter rotor blades, NASA CR-181899.

Chattopadhyay, A. and McCarthy, T. R. (1991). Multiobjective design optimization of helicopter rotor blades with multidisciplinary couplings. In *Optimization of Structural Systems and Industrial Applications* (Edited by S. Hernandez and C. A. Brebbia), pp. 451-462.

Chattopadhyay, A. and McCarthy, T. R. (1993). Multidisciplinary optimization approach for vibration reduction in helicopter rotor blades. *Comput. Math. appl.* **25**(2), 59-72.

Chattopadhyay, A. and Narayan, J. (1992). Optimum design of high speed prop-rotors using a multidisciplinary approach. Presented at the *48th Annual Forum of the American Helicopter Society*, June, Washington, DC.

Chattopadhyay, A., Walsh, J. L. and Riley, M. F. (1991). Integrated aerodynamic/dynamic optimization of helicopter blades. Special Issue of *AIAA J. Aircr.*

Fadel, G. M., Riley, M. F. and Barthelemy, J. M. (1990). Two point exponential approximation method for structural optimization. *Struct. Optimization* **2**, 117–224.

He, C. and Peters, D. A. (1990). Optimization of rotor blades for combined structural, dynamic, and aerodynamic properties. *Proc. Third Air Force/NASA Symp. on Recent Advances in Multidisciplinary Analysis and Optimization*, San Francisco, CA, September.

Johnson, W. (1980). *Helicopter Theory*. Princeton University Press, NJ.

Johnson, W. (1980b). A comprehensive analytical model of rotorcraft aerodynamics and dynamics, part II: user's manual, NASA TM 81183.

Johnson, W. (1988). A comprehensive analytical model of rotorcraft aerodynamics and dynamics—Johnson aeronautics version, vol. II: user's manual.

Lim, J. W. and Chopra, I. (1988). Aeroelastic optimization of a helicopter rotor. *Proc. 44th Annual Forum of the AHS*, June, Washington, DC.

McCarthy, T. R. (1992). An integrated multidisciplinary optimization approach for rotary wing design. Masters Thesis, Arizona State University.

Smith, E. C. and Chopra, I. (1991). Formulation and evaluation of an analytical model for composite box-beams. *J. A.H.S.* **36**(3).

Sobieszczanski-Sobieski, J., Dovi, A. and Wrenn, G. (1988). A new algorithm for general multiobjective optimization, NASA TM-100536, March.

Straub, F., Callahan, C. B. and Culp, J. D. (1991). Rotor design optimization using a multidisciplinary approach, paper no. AIAA 91-0477. Presented at the *29th Aerospace Sciences Meeting*, Reno, Nevada, January.

Vanderplaats, G. N. (1973). CONMIN—A fortran program for constrained function minimization, user's manual, NASA TMX-62282.

Weller, W. H. and Davis, M. W. (1986). Applications of design optimization techniques to rotor dynamics problems. *Proc. 42nd Annual Forum of the AHS*, June, pp. 27–44.